Excitable Greenberg-Hastings cellular automaton model on scale-free networks

An-Cai Wu,[1] Xin-Jian Xu,[2] and Ying-Hai Wang[1,*]
[1]*Institute of Theoretical Physics, Lanzhou University, Lanzhou Gansu 730000, China*
[2]*Departamento de Física da Universidade de Aveiro, 3810-193 Aveiro, Portugal*
(Received 30 September 2006; published 8 March 2007)

We study the excitable Greenberg-Hastings cellular automaton model on scale-free networks. We obtain analytical expressions for no external stimulus the uncoupled case. It is found that the curves, the average activity F versus the external stimulus rate r, can be fitted by a Hill function, but not exactly, there exists a relation $F \sim r^{\alpha}$ for the low-stimulus response, where the Stevens-Hill exponent α ranges from $\alpha=1$ in the subcritical regime to $\alpha=0.5$ at criticality. At the critical point, the range is maximal, but not divergent. We also calculate the average activity $F^k(r)$ and the dynamic range $\Delta^k(p)$ for nodes with given connectivity k. It is interesting that nodes with larger connectivity have larger optimal range, which could be applied in biological experiments to reveal the network topology.

DOI: 10.1103/PhysRevE.75.032901 PACS number(s): 87.10.+e, 87.18.Sn, 05.45.−a

Many systems in the real world, either naturally evolved or artificially designed, are organized in a network fashion [1]. The most-studied networks are the exponential networks in which the node degree distribution [the probability $P(k)$ that a node if connected to other k nodes] is exponentially bounded. A typical model of this network is the Watts-Strogatz (WS) graph [2] which exhibits the small-world phenomenon that was observed in realistic networks [3]. On the contrary, it has been observed recently that the node degree distributions of many real-world networks have power-law tails (scale-free property, due to the absence of a characteristic value for the degrees) $P(k) \sim k^{-\gamma}$ with $2 \leqslant \gamma \leqslant 3$ [4]. There always exists a small number of nodes which are connected to a large number of other nodes in scale-free (SF) networks. This heterogeneity leads to intriguing properties of SF networks. A lot of work has been devoted in the literature to the study of static properties of the networks, while much interest is growing in the dynamical properties of this kind of network. In the context of percolation, SF networks are stable against random removal of nodes while they are fragile under intentional attacks targeting nodes with high degree [5,6]. Also, there are no epidemic thresholds in SF networks [7] and no kinetic effects in reaction-diffusion processes taking place on SF networks [8].

In this Brief Report, we will study the excitable Greenberg-Hastings cellular automaton (GHCA) model [9] on the SF network; especially we focus here on the Barabási and Albert (BA) graph [4]. Due to experimental data which suggest that some classes of spiking neurons in the first layers of sensory systems are electrically coupled via gap junctions or ephaptic interactions [10], the GHCA model has been employed to model the response of the sensory network to external stimuli in some recent work. The two-dimensional deterministic cellular automaton model was studied by computer simulations [11]. Analytical results have recently been obtained for the one-dimensional cellular automaton model under the two-site mean-field approximation [12]. In Ref. [13], Kinouchi and Copelli studied the GHCA model on an Erdös-Rényi random graph (a kind of exponential network) with stochastic activity propagation, and they found as a new and important result that the dynamic range is maximal at the critical point.

In the n-state GHCA model [9] for excitable systems, the instantaneous membrane potential of the ith cell ($i=1,\ldots,N$) at discrete time t is represented by $x_i(t) \in \{0,1,\ldots,n-1\}$, $n \geqslant 3$. The state $x_i(t)=0$ denotes a neuron at its resting (polarized) potential, $x_i(t)=1$ represents a spiking (depolarizing) neuron, and $x_i(t)=2,\ldots,n-1$ accounts for the afterspike refractory period (hyperpolarization). There are two ways for the ith element to go from the state $x_i(t)=0$ to $x_i(t+1)=1$: (a) due to an external signal, modeled here by a Poisson process with rate r [which implies a transition with probability $\lambda=1-\exp(-r\Delta t)$ per time step]; (b) with probability p, due to a neighbor j being in the excited state in the previous time step. If $x_i(t) \geqslant 1$, then $x_i(t+1)=(x_i(t)+1) \bmod n$, regardless of the stimulus. Time is discrete. We assume $\Delta t=1$ ms which corresponds to the approximate duration of a spike and is the time scale adopted for the time step of the model. The number of states n therefore controls the duration of the refractory period (which corresponds to $n-2$, in ms). In the biological context, r could be related, for example, to the concentration of a given odorant presented to an olfactory epithelium [14], or the light intensity stimulating a retina [10]. We shall refer to r as the stimulus rate or intensity.

The BA graph is a kind of SF network and can be constructed according to Ref. [4]. Starting from a small number m_0 of nodes, every time step a new vertex is added, with m links that are connected to an old node i with a probability that is proportional to node i's degree. After iterating this scheme a sufficient number of times, we obtain a network composed of N nodes with degree distribution $P(k) \sim k^{-3}$ and average degree $\langle k \rangle = 2m$. In this Brief Report, we build BA graph with size $N=10^4$ and $m_0=m=4$.

Let $\rho_t(s)$ be the densities of neurons which are in state s at time t. We have the normalization condition $\sum_{s=0}^{n-1} \rho_t(s)=1$. Since the dynamics of the refractory state is deterministic, the equations for $s \geqslant 2$ are simply

*Author to whom correspondence should be addressed. Electronic address: yhwang@lzu.edu.cn

$$\rho_{t+1}(2) = \rho_t(1),$$

$$\rho_{t+1}(3) = \rho_t(2),$$

$$\vdots$$

$$\rho_{t+1}(n-1) = \rho_t(n-2). \tag{1}$$

By imposing the stationarity condition, we have

$$\rho_t(0) = 1 - (n-1)\rho_t(1). \tag{2}$$

Following ideas developed by Pastor-Satorras *et al.* [7], to take into account strong fluctuations in the connectivity distribution, we consider the relative density $\rho_t^k(1)$ of active nodes with given connectivity k by the following equation:

$$\partial_t \rho_t^k(1) = -\rho_t^k(1) + \lambda \rho_t^k(0) + kp(1-\lambda)\rho_t^k(0)\Theta(\rho_t(1)), \tag{3}$$

where $\Theta(\rho_t(1))$ is the probability that any given link points to an active node and is assumed to be a function of the total density of exciting nodes $\rho_t(1)$. In the steady state, $\rho_t(1)$ is just a function of λ and p. Thus, the probability Θ becomes an implicit function of λ and p. By imposing the stationarity condition $\partial_t \rho_t^k(1)=0$, we obtain

$$\rho^k(1) = \frac{\lambda + (1-\lambda)pk\Theta(\lambda,p)}{1 + (n-1)[\lambda + (1-\lambda)pk\Theta(\lambda,p)]}. \tag{4}$$

This set of equations shows that the higher the node connectivity, the higher the probability to be in a spiking state. This inhomogeneity must be taken into account in the computation of $\Theta(\lambda,p)$. Indeed, the probability that a link points to a node with q links is proportional to $qP(q)$. In other words, a randomly chosen link is more likely to be connected to an exciting node with high connectivity, yielding the relation

$$\Theta(\lambda,p) = \sum_k \frac{kP(k)\rho^k(1)}{\sum_q qP(q)}. \tag{5}$$

Since $\rho^k(1)$ is in its turn a function of $\Theta(\lambda,p)$, we obtain a self-consistency equation that allows us to find $\Theta(\lambda,p)$ and an explicit form for Eq. (4). Finally, we can evaluate the order parameter (persistence) $\rho(1)$ using the relation

$$\rho(1) = \sum_k P(k)\rho^k(1). \tag{6}$$

For the BA graph, the full connectivity distribution is given by $P(k)=2m^2k^{-3}$, where m is the minimum number of connection at each node. By noticing that the average degree is $\langle k\rangle = \int_m^\infty kP(k)dk = 2m$, Eq. (5) gives

$$\Theta(\lambda,p) = m\int_m^\infty \frac{dk}{k^2} \frac{\lambda + (1-\lambda)pk\Theta(\lambda,p)}{1 + (n-1)[\lambda + (1-\lambda)pk\Theta(\lambda,p)]}, \tag{7}$$

which yields the solution

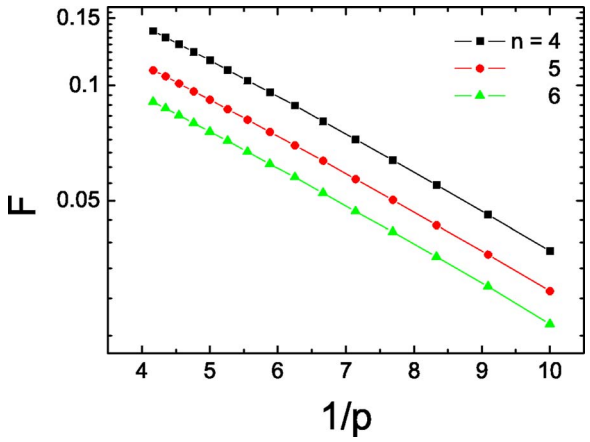

FIG. 1. (Color online) In the absence of stimulus, the average activity F as a function of $1/p$. The linear behavior on the semilogarithmic scale proves the exponential behavior predicted by Eq. (10).

$$\Theta(\lambda,p) = \frac{\lambda}{b} + \left(\frac{\lambda}{b} - \frac{1}{n-1}\right)\frac{ma\Theta(\lambda,p)}{b} \ln \frac{ma\Theta(\lambda,p)}{ma\Theta(\lambda,p)+b}, \tag{8}$$

where $a=(n-1)(1-\lambda)p$ and $b=1+(n-1)\lambda$. We can solve the above equation to obtain the solution $\Theta(\lambda,p)$. Theoretically, combining Eqs. (4), (6), and (8), we can obtain the final result of $\rho(1)$. In some special cases the analytical expressions can be obtained.

(i) No external stimulus, i.e., $\lambda=0$ or $r=0$. We can obtain

$$\Theta(0,p) = \frac{e^{-1/mp}}{(n-1)mp}(1-e^{-1/mp})^{-1}. \tag{9}$$

Combining Eqs. (4), (6), and (9), we find the solution for the density of active nodes when there is no external stimulus,

$$\rho(1) \sim \frac{1}{n-1}e^{-1/mp}. \tag{10}$$

(ii) The uncoupled case, i.e., $p=0$. Combining Eqs. (4) and (6), we have

$$\rho(1) = \frac{\lambda}{1+(n-1)\lambda}, \tag{11}$$

which is independent of the network's topology, so it has also been obtained in other networks, such as the one-dimensional case [12]. When the external stimulus intensity r is very small, $\rho(1)\sim r^{-1}$.

We define the average activity

$$F = \frac{1}{T}\sum_{t=1}^{T} \rho_t(1), \tag{12}$$

where T is a large time window (of the order of 10^4 time steps). In the stationary state, it is obvious that $F=\rho(1)$. To confirm the picture extracted from the above analytic treatment, we perform numerical simulations on the BA network. Figure 1 shows the behavior of the average activity F in the absence of stimulus. All the plots decay with an exponent

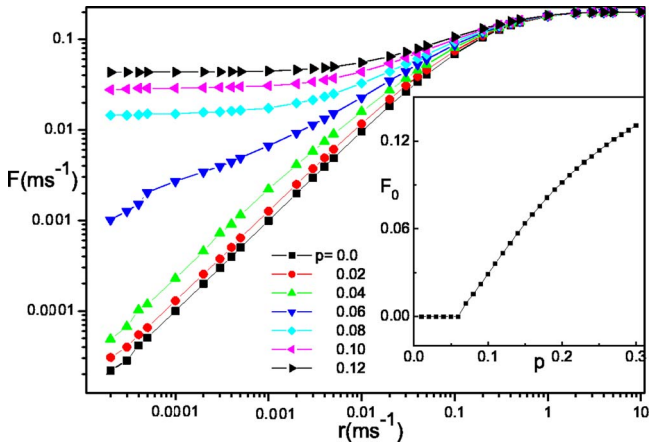

FIG. 2. (Color online) Response curves (mean firing rate F vs stimulus rate r). Points represent simulation results with $n=5$ states and $T=10^3$ ms, from $p=0$ to 0.12 (in intervals of 0.02). These curves are power laws $F \propto r^{\alpha}$ with $\alpha=1$ (subcritical) and 1/2 (critical). Inset: Spontaneous activity F_0 vs branching probability p; the critical point is $p_c=0.06$.

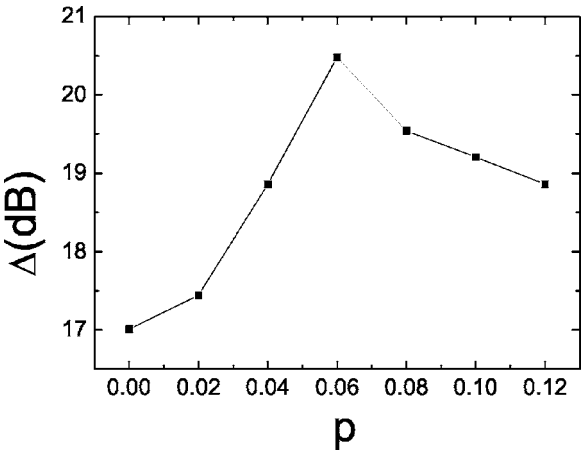

FIG. 3. Dynamic range Δ vs branching probability p. The curve is obtained by calculating the data from Fig. 2. There is a finite maximal range precisely at the critical point $p_c=0.06$.

form $F \sim \exp(-c/mp)$, where c is a constant. The numerical value obtained, $c=0.226$, is in good agreement with the theoretical prediction of Eq. (10), $c=1/m=0.25$.

In Fig. 2, we show the average activity F versus the external stimulus rate r for different branching probability p. The inset shows the spontaneous activity F_0 versus the branching probability p in the absence of stimulus ($r=0$). There is a critical point $p_c=0.06$; only at $p>p_c$ is there a self-sustained activity, $F>0$. We perform numerical simulations on BA graphs with different system sizes and find that the value of p_c reduces to zero as the system size N increases. The curves $F(r)$ could be fitted by a Hill function $F(r)=F_{max}r^{\alpha}/(c^{\alpha}+r^{\alpha})$, where c is the stimulus rate for half maximum response, but are not exactly Hill functions, and there exists the relation $F \sim r^{\alpha}$ for the low-stimulus response. It is found that the Stevens-Hill exponent α changes from $\alpha=1$ in the subcritical regime to $\alpha=0.5$ at criticality. This important point was also reported by Ref. [13] where the network is an Erdös-Rényi random graph. We also notice that apparent exponents between 0.5 and 1.0 are observed [12] if finite size effects are present, that is, if N is small.

As a function of the stimulus intensity r, networks have a minimum response F_0 (=0 for the subcritical and critical cases) and a maximum response F_{max} (due to the absolute nature of the refractory period, $F_{max}=1/n$, which can be obtained by setting $\lambda=1$ in Eq. (11)). Reference [13] defines the dynamic range $\Delta=10\log_{10}(r_{0.9}/r_{0.1})$ as the stimulus interval (measured in decibels) where variations in r can be robustly coded by variations in F, discarding stimuli that are too weak to be distinguished from F_0 or too close to saturation. The range $[r_{0.1}, r_{0.9}]$ is found from its corresponding response interval $[F_{0.1}, F_{0.9}]$, where $F_x=F_0+x(F_{max}-F_0)$.

Figure 3 depicts the dynamic range Δ versus the branching probability p. There is a pronounced finite maximum precisely at the critical point. This result was also found in an Erdös-Rényi random graph [13]. Kinouchi and Copelli explained the result as follows: "In the subcritical regime, sensitivity is enlarged because weak stimuli are amplified due to activity propagation among neighbors. As a result, the dynamic range $\Delta(p)$ increases monotonically with p. In the supercritical regime, the spontaneous activity F_0 masks the presence of weak stimuli, therefore $\Delta(p)$ decreases. The optimal regime occurs precisely at the critical point" [13]. We also perform simulations on other complex networks, such as WS networks and random SF networks with different γ [15], and obtain the same behavior of the average activity F as shown in Fig. 2, the optimal regime occurring precisely at the critical point. We state that this phenomenon represents a universal behavior of the excitable GHCA model on complex networks and the explanation provided by Kinouchi and Copelli is also suitable for other types of complex networks. Furthermore, we perform computer simulations on SF networks with average degree $\langle k \rangle=8$ and degree exponent $\gamma=2.2, 2.5, 3.5$, and obtain that their optimal dynamic ranges are approximately 19.21, 20.01, 21.54, respectively, which means that the more heterogeneous the SF network is, the smaller optimal dynamic range it has.

In SF networks, there exist strong fluctuations in the connectivity distribution. It is worth investigating the behavior of the average activity F^k for nodes with given connectivity k. In Fig. 4 we plot the quantity F^k versus the external stimulus intensity r for different branching probability p. Figures 4(a) and 4(b) correspond to the node connectivity $k=4$ and 36, respectively. It is found that the curves $F^k(r)$ have similar properties as $F(r)$ which was shown in Fig. 2, i.e., the Stevens-Hill exponent α changes from $\alpha=1$ in the subcritical regime to $\alpha=0.5$ at criticality.

Finally, we calculate the dynamic range $\Delta^k(p)$ of nodes with given connectivity k, and the result is shown in Fig. 5. The phenomenon that the optimal regime occurs precisely at the critical point recurs. It is notable that the optimal dynamic range for nodes with given connectivity k increases with k, i.e., nodes with larger connectivity have larger optimal range. One can investigate every node's optimal dynamic range and calculate their fluctuations, since the fluctuations of the node's optimal dynamic range reflect the fluctuations of the node's connectivity in the network. To

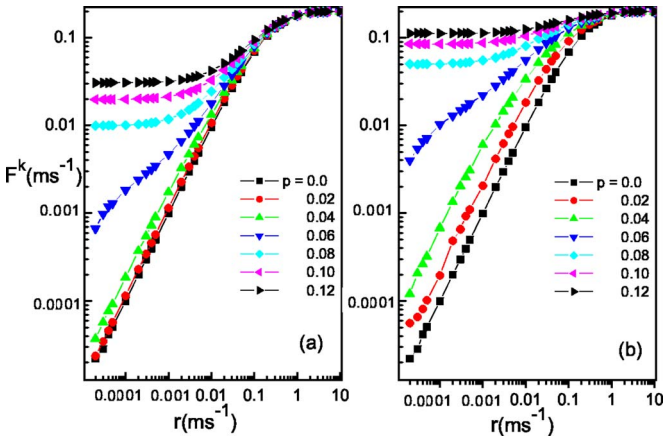

FIG. 4. (Color online) Average activity F^k for nodes with given connectivity k vs external stimulus rate r; for connectivity $k=$(a) 4 and (b) 36. Simulations are performed with $n=5$ states and $T=10^4$ ms, from $p=0$ to 0.12 (in intervals of 0.02). These curves are power laws $F^k \propto r^\alpha$ with $\alpha=1$ (subcritical) and 1/2 (critical).

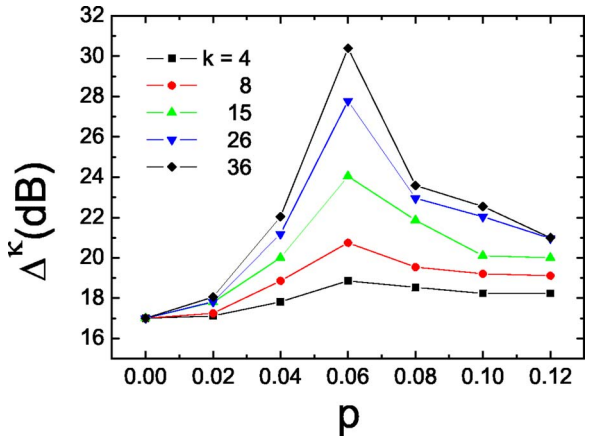

FIG. 5. (Color online) Dynamic range $\Delta^k(p)$ of nodes with given connectivity k vs branching probability p. Points represent the results calculated from simulation with $n=5$ states and $T=10^4$ ms. Dynamic range $\Delta^k(p)$ is optimized at the critical point $p_c=0.06$, although the connectivity k is different.

some extent, we can discover the topology of the network by investigating the dynamics on it.

In summary, we have investigated the behavior of the excitable GHCA model [9] on BA networks. It was found that the curves of the average activity F as a function of the external stimulus rate r can be fitted by a Hill function, but are not exactly Hill functions, and there exists a relation $F \sim r^\alpha$ for the low-stimulus response. The Stevens-Hill exponent α changes from $\alpha=1$ in the subcritical regime to $\alpha=0.5$ at criticality. There is a maximal range precisely at the critical point. We also observed these results numerically in other kinds of complex networks. We conclude that these phenomena represent a universal behavior of the excitable GHCA model on complex networks. Due to strong fluctuations in the connectivity distribution on the BA graph, we calculated the average activity $F^k(r)$ and the dynamic range $\Delta^k(p)$ for nodes with given connectivity k. The two quantities $F^k(r)$ and $\Delta^k(p)$ have similar behavior to that of $F(r)$ and $\Delta(p)$, respectively. It is interesting that nodes with larger connectivity have larger optimal range. This property could be applied in biological experiments, revealing the network topology.

This work was supported by the Fundamental Research Fund for Physics and Mathematics of Lanzhou University under Grant No. Lzu05008. X.-J.X. acknowledges financial support from FCT (Portugal), Grant No. SFRH/BPD/30425/2006.

[1] R. Albert and A.-L. Barabási, Rev. Mod. Phys. **74**, 47 (2002); S. N. Dorogovtsev and J. F. F. Mendes, Adv. Phys. **51**, 1079 (2002); M. E. J. Newman, SIAM Rev. **45**, 167 (2003).
[2] D. J. Watts and S. H. Strogatz, Nature (London) **393**, 440 (1998).
[3] D. J. Watts, *Small Worlds: The Dynamics of Networks Between Order and Randomness* (Princeton University Press, Princeton, NJ, 1999).
[4] A.-L. Barabási and R. Albert, Science **286**, 509 (1999); A.-L. Barabási, R. Albert, and H. Jeong, Physica A **272**, 173 (1999).
[5] R. Albert, H. Jeong, and A.-L. Barabási, Nature (London) **406**, 378 (2000).
[6] R. Cohen, K. Erez, D. ben-Avraham, and S. Havlin, Phys. Rev. Lett. **85**, 4626 (2000).
[7] R. Pastor-Satorras and A. Vespignani, Phys. Rev. Lett. **86**, 3200 (2001); Phys. Rev. E **63**, 066117 (2001); **65**, 036104 (2002).
[8] L. K. Gallos and P. Argyrakis, Phys. Rev. Lett. **92**, 138301 (2004).
[9] J. M. Greenberg and S. P. Hastings, SIAM J. Appl. Math. **34**, 515 (1978).
[10] M. R. Deans, B. Volgyi, D. A. Goodenough, S. A. Bloomfield, and D. L. Paul, Neuron **36**, 703 (2002).
[11] M. Copelli and O. Kinouchi, Physica A **349**, 431 (2005).
[12] L. S. Furtado and M. Copelli, Phys. Rev. E **73**, 011907 (2006).
[13] O. Kinouchi and M. Copelli, Nat. Phys. **2**, 348 (2006).
[14] J.-P. Rospars, P. Lánský, P. Duchamp-Viret, and A. Duchamp, BioSystems **58**, 133 (2000).
[15] S. N. Dorogovtsev, J. F. F. Mendes, and A. N. Samukhin, Phys. Rev. Lett. **85**, 4633 (2000).